Convergence to equilibrium in a class of interacting particle systems evolving in discrete time

Henryk Fukś [a] and Nino Boccara [b]

[a] *Department of Mathematics*
Brock University
St. Catharines, Ontario L2S 3A1,
Canada
`hfuks@brocku.ca`
and
The Fields Institute for Research
in Mathematical Sciences
Toronto, Ontario M5T 3J1, Canada

[b] *Department of Physics, University of*
Illinois at Chicago, Chicago, IL
60607-7059, USA
`boccara@uic.edu`
and
DRECAM/SPEC, CE Saclay, 91191
Gif-sur-Yvette Cedex, France

Abstract

We conjecture that for a wide class of interacting particle systems evolving in discrete time, namely conservative cellular automata with piecewise linear flow diagram, relaxation to the limit set follows the same power law at critical points. We further describe the structure of the limit sets of such systems as unions of shifts of finite type. Relaxation to the equilibrium resembles ballistic annihilation, with "defects" propagating in opposite direction annihilating upon collision.

1. Introduction

Interacting particle systems evolving in discrete time have found many applications in recent years, especially in the field of road traffic modeling (see [1] and references therein). While majority of traffic models based on interacting particle systems are stochastic, some features of the real traffic flow may be well described by purely deterministic models, as reported in [2, 3, 4].

An important characterization of a system of interacting particles is its fundamental diagram, *i.e.*, the graph of the particle flux through a fixed point, in the equilibrium state, as a function of particle density. In many cases, such diagrams exhibit a discontinuity of the first derivative, and are very often piecewise linear. In the simplest cases there is only one such a discontinuity, and the fundamental diagram has the shape of an inverted "V". Linear segments of the diagram can be interpreted as distinct "phases."

The discontinuity of the first derivative, to be further called a critical point, displays many features similar to critical phenomena known in statistical physics. The phenomenon of critical slowing down is especially apparent: when the density of particles approaches the critical density, the convergence to the equilibrium becomes slower. In what follows, we will present an evidence which strongly suggests that at the critical point the rate of convergence follows a power law with a universal exponent equal to $-\frac{1}{2}$.

2. Interacting particle systems and cellular automata

Discrete version of a totally asymmetric exclusion process is a simple yet often studied example of interacting particle system.[5, 6, 7, 8, 9] The dynamics of this process can be described as follows: particles reside on a one-dimensional lattice, with at most one particle per site. At each time $t \in \mathbf{N}$, each particle checks if the site to the right of its current position is empty, and if it is, it jumps to this site. The process is synchronous, meaning that all particles jump at the same time.

Two alternative descriptions of this process are possible. We can label each particle with an integer $n \in \mathbf{Z}$, such that the closest particle to the right of particle n is labeled $n + 1$. If $s(n, t)$ denotes the position of particle n at time t, the configuration of the particle system at time t is described by the increasing bisequence $\{s(n,t)\}_{n=-\infty}^{\infty}$. The dynamics of the totally asymmetric exclusion process can be now stated as

$$s(n, t + 1) = s(n, t) + \min\{s(n + 1, t) - s(n, t) - 1, 1\}. \tag{1}$$

Another possible approach is to describe the process in the language of cellular automata. If lattice sites are labeled with consecutive integers $i \in \mathbf{Z}$, defining $x(i, t) = 1$ if the site i is occupied by a particle, and $x(i, t) = 0$ if it is empty, the configuration of the particle system at time t is, in this case, described by the bisequence $\{x(i,t)\}_{i=-\infty}^{\infty}$. One can easily show that the dynamics of the aforementioned process is then given by

$$x(i, t + 1) = f\Big(x(i - 1, t), x(i, t), x(i + 1, t)\Big), \tag{2}$$

where f is defined by

$$f(0, 0, 0) = 0, \ f(0, 0, 1) = 0, \ f(0, 1, 0) = 0, \ f(0, 1, 1) = 1 \tag{3}$$
$$f(1, 0, 0) = 1, \ f(1, 0, 1) = 1, \ f(1, 1, 0) = 0, \ f(1, 1, 1) = 1.$$

The above definition can also be written in a more compact form as

$$x(i, t + 1) = x(i, t) + \min\{x(i - 1, t), 1 - x(i, t)\} - \min\{x(i, t), 1 - x(i + 1, t)\}. \tag{4}$$

The evolution rule (4) is often called cellular automaton rule 184, using the numbering scheme introduced by Wolfram [10].

Consider now the general cellular automaton:

$$x(i, t + 1) = f\Big(x(i - r_l, t), x(i - r_l + 1, t), \dots, x(i + r_r, t)\Big), \tag{5}$$

where the function $f : \{0,1\}^{r_l+r_r+1} \mapsto \{0,1\}$ is the evolution rule of the automaton, and the positive integers r_l and r_r are, respectively, the left and right radius of the rule. f will also be called a k-input rule where $k = r_l + r_r + 1$ is the number of arguments of f. A rule f is said to be conservative if for any periodic configuration of period L (*i.e.*, a configuration such that $x(i+L,t) = x(i)$ for every $i \in \mathbf{Z}$) we have

$$\sum_{i=1}^{L} x(i,t+1) = \sum_{i=1}^{L} x(i,t). \tag{6}$$

Every conservative cellular automaton rule can be viewed as the evolution rule of a system of interacting particles, just like rule 184 defined above, and a configuration of such a system can be represented by an increasing bisequence $\{s(n,t)\}_{n=-\infty}^{\infty}$, where $s(n,t)$ denotes the position of particle n at time t. A formal proof of this statement and an algorithm for construction of an analog of equation (1) for a given conservative rule f can be found in [11]. In [12] we have presented a survey of 4-input and 5-input conservative cellular automata rules and their properties.

In order to describe the motion of the particles, we will use a visual representation of rule f constructed as follows. List all relevant neighborhood configurations of a given particle represented by 1. Then, for each neighborhood, indicate the displacement of this particle drawing an arrow joining the initial and final positions of the particle. For rule 184, this would be

$$\overset{\frown}{10}, \quad \overset{\circlearrowleft}{11}, \tag{7}$$

where a circular arrow indicates that the particle does not move. The above notation is equivalent to saying that all particles which have empty sites immediately to their right jump one site to the right, while other particles do not move.

We will normally list only neighborhoods resulting in particle motion, assuming that by default, in all other cases, particles do not move. Rule 184, for example, we will simply represented by $\overset{\frown}{10}$.

All particles do not necessarily move in the same direction. For example, there could be a process such that a particle will move one site to the right when the two nearest neighboring sites on its right are empty while, if its right neighboring site is occupied and its left neighboring site is empty, the particle moves one site to the left. In all other cases, the particle remains immobile. This rule can be visually represented by

$$\overset{\frown}{100}, \quad \overset{\frown}{011}. \tag{8}$$

The main quantities of interest in this paper are the average particle velocity and flux at time t. For a periodic configuration of period L, the average velocity is defined as

$$v(t) = \frac{1}{N} \sum_{n=1}^{N} \big(s(n,t-1) - s(n,t)\big), \tag{9}$$

where N is the number of particles in a single period. The flux is defined as $\phi(t) = \rho v(t)$, where $\rho = N/L$ is the density of particles. In what follows, we assume that, at $t = 0$,

3

particles are randomly distributed on the lattice. When $L \to \infty$, this corresponds to the Bernoulli product measure on $\mathbf{Z}$, with lattice sites occupied by a particle with probability ρ, and empty with probability $1 - \rho$. If $b = b_1 b_2 \ldots b_k$ is a block of finite length k, where, for all $i \in \{1, 2, \ldots, k\}$ $b_i \in \{0, 1\}$, the probability of occurrence of block b in the configuration $\{x(i,t)\}_{i=-\infty}^{\infty}$ will be denoted by $P_t(b)$.

3. Exact solution for deterministic traffic rule

A natural extension of the totally asymmetric exclusion process with discrete time has been studied in connection with traffic models [13]. Each site is either occupied by a particle, or empty. The velocity of each particle is an integer between 0 and m. As before, if $s(n,t)$ denotes the position of the nth car at time t, the position of the next car ahead at time t is $s(n+1,t)$. With this notation, the system evolves according to a synchronous rule given by

$$s(n, t+1) = s(n,t) + v(i,t), \tag{10}$$

where

$$v(n,t) = \min\{s(n+1,t) - s(n,t) - 1, m\} \tag{11}$$

is the velocity of the particle n at time t. Since $g = s(n+1,t) - s(n,t) - 1$ is the gap (number of empty sites) between particles n and $n+1$ at time t, one could say that each time step, each particle advances by g sites to the right if $g \leq m$, and by m sites if $g > m$. When $m = 1$, this model is equivalent to elementary cellular automaton rule 184 discussed in the previous section.

If we start with a random initial ($t = 0$) configuration with particle density ρ, it is possible to obtain an exact expression for the flux at a later time $t > 0$, as shown in [14]:

$$\phi(t) = 1 - \rho - \sum_{j=1}^{t+1} \frac{j}{t+1} \binom{(m+1)(t+1)}{t+1-j} \rho^{t+1-j}(1-\rho)^{m(t+1)+j}. \tag{12}$$

In the limit $t \to \infty$, we obtain the flux $\phi(\infty)$ at equilibrium which is the piecewise linear function of ρ defined by

$$\phi(\infty) = \begin{cases} m\rho & \text{if } \rho < 1/(m+1), \\ 1 - \rho & \text{otherwise.} \end{cases} \tag{13}$$

We can see that for $\rho < 1/(m+1)$ the average velocity of particles at equilibrium is m, *i.e.*, all particles are moving to the right with maximum speed m. The system is said to be in the *a free-moving phase*. When $\rho > 1/(m+1)$, the speed of some particles is less than the maximum speed m. The system is in the so-called *jammed phase*.

The transition from the free-moving phase to the jammed phase occurs at $\rho = \rho_c = 1/(m+1)$ called the *critical density*. At ρ_c, it is possible to obtain an asymptotic approximation of (12) by replacing the sum by an integral and using de Moivre-Laplace limit theorem, as done in [14]. At ρ_c this procedure yields

$$\phi(\infty) - \phi(t) = \sqrt{\frac{m}{2\pi(m+1)t}} \left(e^{-\frac{(m+1)}{2mt}} - e^{-\frac{(m+1)t}{2m}} \right), \tag{14}$$

4

Rule nr	Motion representation
3213933712	$01\overparen{01}\ 1\overparen{10}\ 1\overparen{10}$
3482385552	$01\overparen{01}\ 01\overparen{10}\ 1\overparen{10}$
3486567632	$01\overparen{01}\ 1\overparen{10}$
3163339916	$1\overparen{10}$
3487613920	$01\overparen{00}\ 1\overparen{10}$
3167653058	$00\overparen{01}\ 11\overparen{10}$

Table 1: Examples of conservative rules with piecewise linear fundamental diagrams

or, in other words, $\phi(\infty) - \phi(t) \sim t^{-1/2}$. Here, by $f(t) \sim g(t)$ we mean that $\lim_{t\to\infty} f(t)/g(t)$ exists and is different from 0. Power law convergence to the equilibrium at the critical point for rule 184 has been established in [5] and [15].

In the next section we will present some numerical results suggesting that this behavior is universal for a wide class of interacting particle systems evolving in discrete time.

4.   Numerical results for other CA rules

Among conservative 5-input cellular automata rules investigated in [12], a majority exhibit piecewise linear fundamental diagrams (*i.e.*, graphs of $\phi(\infty)$ as a function of ρ). For the purpose of this article, we have selected six representative examples of such rules among the 428 conservative 5-input rules. These six rules are given in Table 1, and their fundamental diagrams are shown in Figure 1. Points at which the slope of the fundamental diagram changes are referred to as critical points. In Figure 1, there are three rules with a single critical point, and whose fundamental diagrams are similar to rule 184. The remaining three rules have, respectively, 2, 3, and 4 critical points.

In order to illustrate that at a critical point, as a function of time t, the system converges to equilibrium as $t^{-1/2}$, we define the decay time as

$$\tau = \sum_{t=0}^{\infty} |\phi(t) - \phi(\infty)|. \tag{15}$$

If the decay is of power-law type, the above sum diverges.

For all rules in Table 1, we have performed computer simulations to estimate τ. Results are shown in Figure 2, where τ is plotted as a function of density for each rule. The value of τ has been estimated by measuring $\phi(t)$ for $t = 0, 1, \ldots, 1000$, and truncating the sum (15) at $t = 1000$. Comparing Figures 1 and 2 we clearly see that τ diverges at critical points. In order to verify that indeed $|\phi(\infty) - \phi(t)| \sim t^{-1/2}$ at critical points, we have plotted (for all critical points) the numerical values of $|\phi(\infty) - \phi(t)|$ as a function of t using logarithmic coordinates. Figure 3 shows an example of such a graph, for the critical point of the first rule in Table 1 (code number: 3213933712). The (ρ, ϕ) coordinates of this critical point in the fundamental diagram are $(\frac{2}{3}, \frac{2}{3})$. Assuming that $|\phi(\infty) - \phi(t)| \sim t^{-\alpha}$, we have
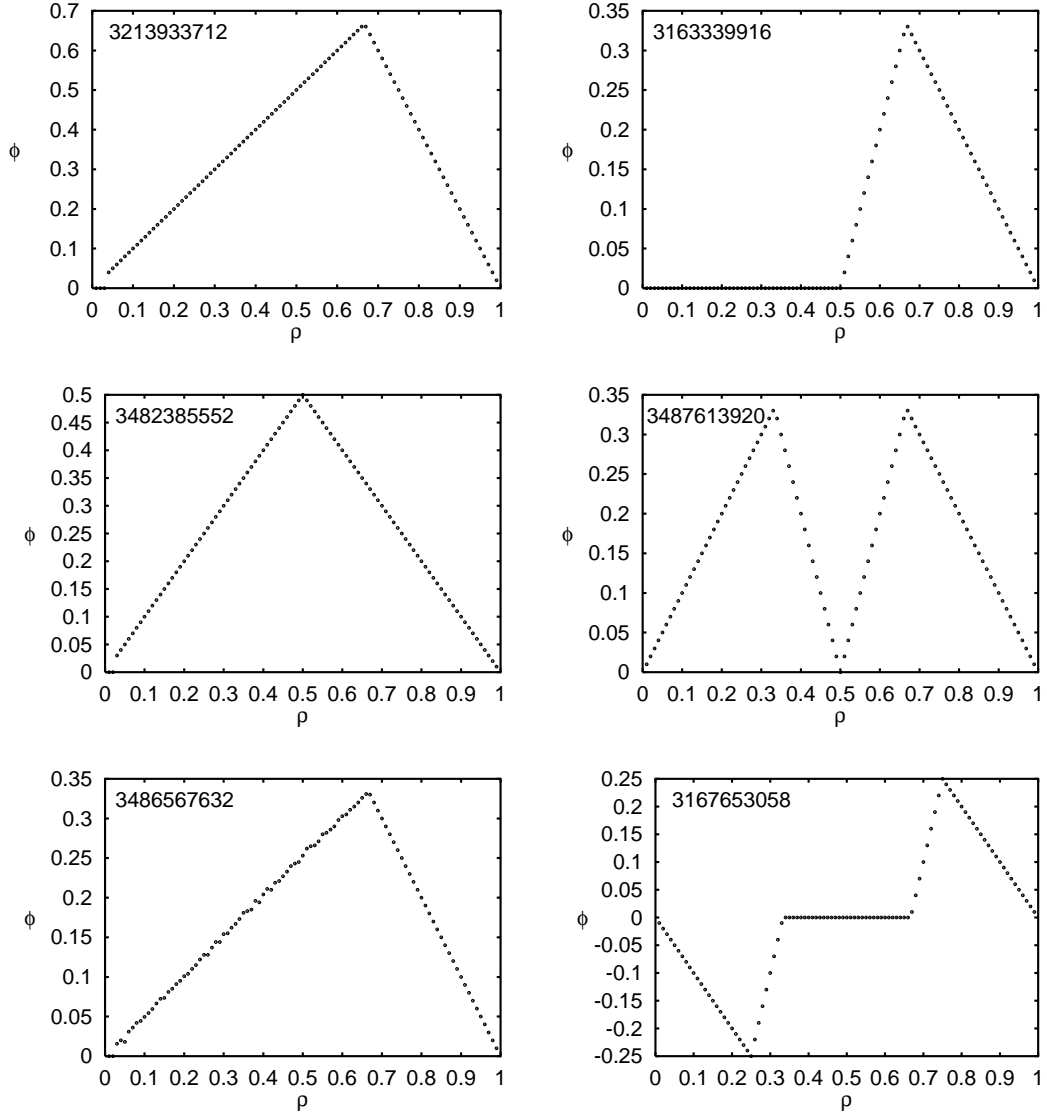
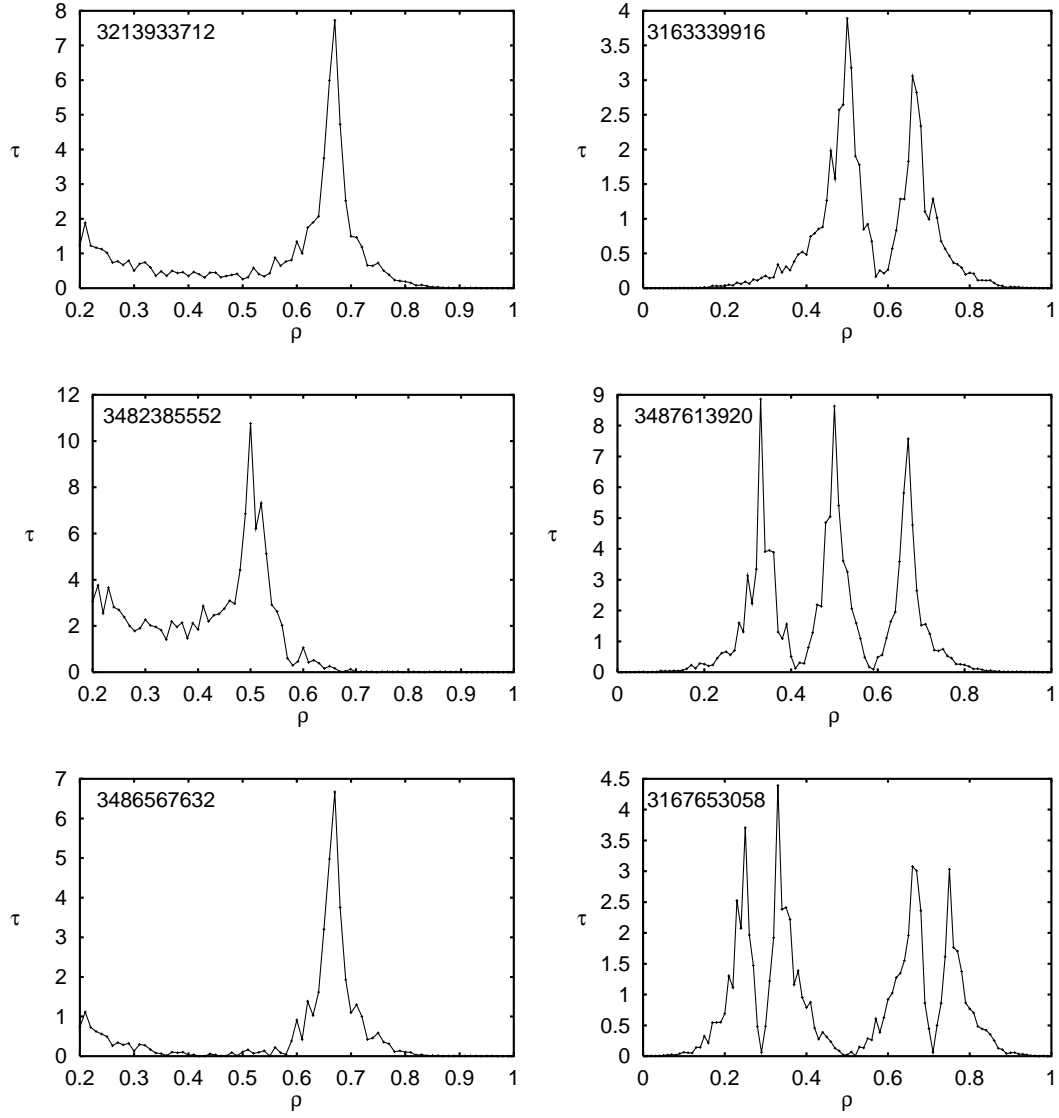Figure 1: Fundamental diagrams for rules from Table 1.

Figure 2: Decay time as a function of density for rules from Table 1.
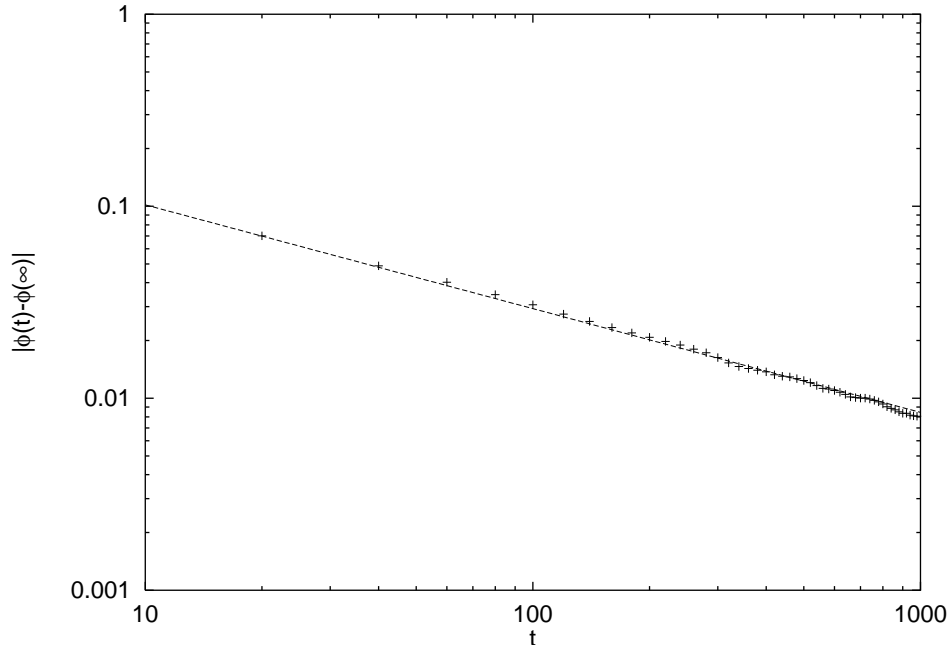
Figure 3: Logarithmic plot of $|\phi(\infty) - \phi(t)|$ as a function of t for rule 3213933712. Data points (+) represent computer simulations, while the dashed line represents the best fit (slope $= -0.501 \pm 0.01$)

determined the exponent α as the slope of the straight line which best fit the logarithmic plot of $|\phi(\infty) - \phi(t)|$. Table 2 shows our results for all the critical points of all the six rules of Table 1. All these exponents are remarkably close to $\frac{1}{2}$, suggesting that $t^{-1/2}$ might be a universal law governing the rate of convergence to equilibrium at critical points of conservative cellular automata with piecewise linear fundamental diagrams.

5.   Shifts of finite type

In order to understand why the decay to equilibrium, or, in other words, approach to the limit set follows the same law for different rules, we now describe limit sets of conservative rules using the concept of a *shift of finite type* (SFT). In symbolic dynamics and coding theory [16], SFT is defined as follows: let B be a finite set of finite blocks (consecutive sites), *e.g.* $B = \{00, 11, 101\}$. Consider a set of all bi-infinite configurations in which blocks of the set B do not appear ("forbidden blocks"). Such a set, denoted by $\text{SFT}(B)$, is called a shift of finite type.

By analyzing frequencies of occurrences of finite blocks in conservative CA, one can observe that limit sets of many conservative CA are unions of two or more SFT's. Each of these SFT's correspond to a distinct "phase", or a straight line segment in the fundamental diagram. Critical points correspond to a set of configurations common to two SFT's. Forbidden block sets of each phase completely determine the fundamental diagram.

As an example, consider the deterministic traffic rule defined by the relations (10) and

Rule nr	Critical point (ρ, ϕ)	α
3213933712	$(2/3, 2/3)$	0.501
3482385552	$(1/2, 1/2)$	0.517
3486567632	$(2/3, 1/3)$	0.507
3163339916	$(1/2, 0)$	0.506
	$(2/3, 1/3)$	0.504
3487613920	$(1/3, 1/3)$	0.502
	$(1/2, 0)$	0.539
	$(2/3, 1/3)$	0.504
3167653058	$(1/4, -1/4)$	0.486
	$(1/3, 0)$	0.514
	$(2/3, 0)$	0.514
	$(3/4, 1/4)$	0.486

Table 2: Values of the exponent α at critical points of rules from Table 1. Simulations performed using a lattice size equal to 5×10^5.

(11), assuming $m = 2$. We mentioned that in the free-moving phase, all particles move with maximum speed $m = 2$, which implies that 1's are always separated by two or more 0's. Hence, the blocks 11 and 101 cannot be found in a configuration belonging to the limit set of the free-moving phase. In the jammed phase, on the other hand, blocks of zeros of length 3 or more cannot occur. The limit sets of these two phases are therefore, respectively, SFT(11, 101) and SFT(000). Note that these two sets are not completely disjoint, but have three common elements, namely, ...100100100100..., ...001001001001..., and ...010010010010...

Consider now the phase $P1 = $ SFT(11, 101). It is clear that, for any configuration in $P1$, $\rho \leq 1/3$, since two ones must be always separated by two or more zeros. We know that the flow for the above rule is defined as $\phi(t) = 2P(100) + P(101)$. We also know that $P(11) = P(101) = 0$. The consistency condition gives $P(100) + P(101) + P(110) + P(111) = \rho$. Hence, $P(100) = \rho$, and, in this phase, $\phi(\infty) = 2\rho$.

In phase $P2 = $ SFT(000), $P(000) = 0$, and one can show that $\phi(\infty) = 1 - \rho - P(000)$. The proof can be found in [14] (it involves manipulations of the consistency conditions only). Hence, $\phi = 1 - \rho$. In $P2$, the largest number of zeros separating two ones is 2, hence the minimum value of the density ρ is $\frac{1}{3}$, so $\phi(\infty) = 1 - \rho$ is valid for all $\rho \geq \frac{1}{3}$.

Note that we derived the fundamental diagram given by equation (13) from the structure of the limit set only. This can be done for all conservative CA with piecewise linear fundamental diagrams. As mentioned earlier, different straight line segments of the fundamental diagram correspond to different SFT components of the limit set, while configurations common to two SFT's define critical points.

At the critical point, the limit set consists of a finite number of configurations, yet there is an infinite number of initial configurations with a given density. Time evolution of the system governed by a conservative rule can, therefore, be viewed as a transition form an infinite configuration space to a finite configuration space. While details of this transition

are different for different rules, it appears that the rate of convergence follows always the same law, as argued in the previous section.

In order to test this interpretation of the dynamics of conservative CA, we have determined the spatial measure entropy of configurations at time t. The spatial measure entropy of a limit set configuration is defined as

$$s(k) = -\frac{1}{k} \sum_{b \in \{0,1\}^k} P_\infty(b) \log P_\infty(b), \tag{16}$$

where the sum runs over all blocks of length k, and $P_\infty(b)$ denotes the probability of occurrence of block b in the limit set. If, at a given ρ, the number of configurations in the limit set is finite, $s(k)$ should go to zero with $k \to \infty$. Figure 4 shows $s(10)$ plotted as a function of the density ρ for all the six rules of Table 1. Comparing Figures 1 and 4, one can easily notice that, at critical points of fundamental diagrams, $s(10)$ takes minimum values, confirming our observations regarding the structure of limit sets.

6.   Annihilation of defects

The dynamics of rule 184 can be described in terms of soliton-like localized structures propagating in periodic background [17] More formally, it can be shown that rule 184 is equivalent to ballistic annihilation process [18]. This equivalence has been used in [9], and investigated in detail in [15]. The ballistic annihilation process involves two types of particles moving, on a line, at constant speed in opposite directions. When two particles collide, they annihilate. Using the central limit theorem, Elskens and Frisch [18] demonstrated that if the initial distribution of particles is balanced, then, the fraction $S(t)$ of surviving particles at time t behaves as $t^{-1/2}$.

For rule 184, the "background" on which the defects are moving are periodic configurations of alternating zeros and ones, $\ldots 01010101 \ldots$. If we call A-type defect consecutive 1's, and B-type defect two consecutive 0's, it is easy to show [9] that, for each iteration of rule 184, defects type A move to the left, while defects of type B move to the right. When they collide, the reaction $A + B \to background$, i.e., annihilation, takes place.

A very similar construction can be made for the process defined by equation (10) and (11). Here, the background consists of ones separated by m zeros. We can also define two types of defects, but with an additional subscript identifying their length. If two consecutive 1's are separated by a cluster of zeros of length $m + k$ ($k > 0$), this is the defect of type B, denoted B_k. Similarly, if two 1's are separated by a cluster of zeros of length $m - l$ ($m > l > 0$), such a cluster constitutes an A-type defect, denoted A_l. A-type defects move to the left with speed 1 while B-type defects move to the right with speed m. A collision between defects A_l and B_k results in a defect A_{l-k} if $l > k$, and B_{k-l} if $k > l$. If $k = l$, the two defects annihilate. Figure 5 shows an example of such collisions.

The dynamics of other conservative rules with piecewise linear fundamental diagrams can also be interpreted as interaction of defects propagating in a periodic background. However, the number of different types of "defects" and "backgrounds" is typically larger than in the simple cases described above. This can be seen in Figure 6, which shows spatiotemporal
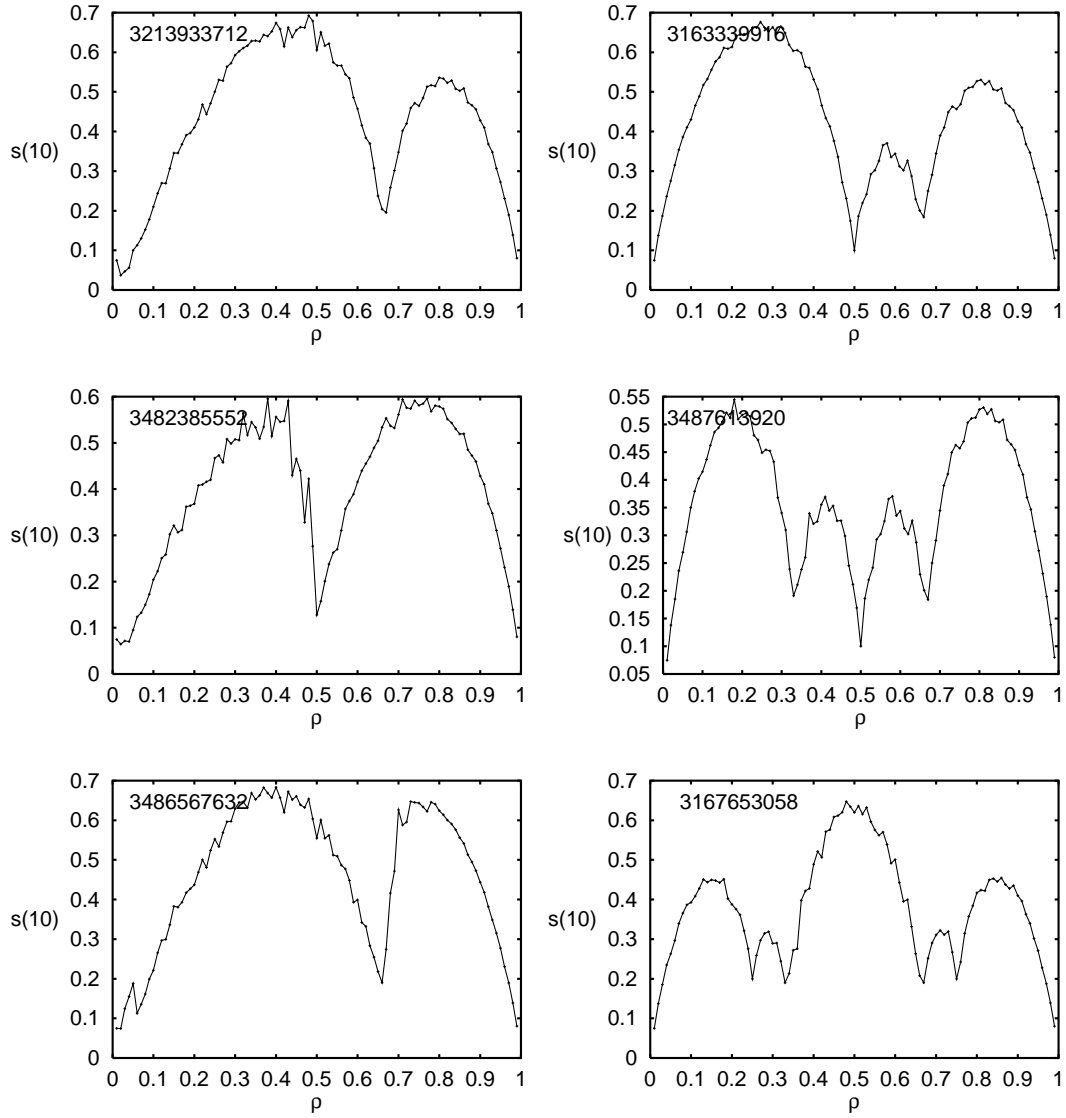
Figure 4: Spatial measure entropy for block length $k = 10$ as a function of density for rules of Table 1.
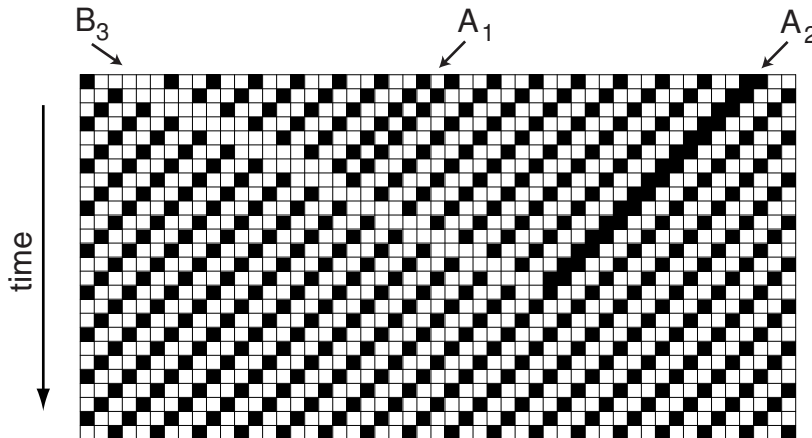
Figure 5: Collision of defects in deterministic traffic rule defined by relations (10) and (11) with $m = 2$. Black squares represent lattice sites occupied by a particle. First, A_1 collides with B_3, resulting in B_2. Several iterations later, B_2 collides with A_2, and both defects disappear.

diagrams for rule 31633399164 $(1\widehat{1}0)$ at $\rho = \frac{1}{2}$ and $\rho = \frac{2}{3}$. "Defects" propagating in opposite directions and annihilating upon collision can be clearly identified in both diagrams. At $\rho = \frac{1}{2}$ all defects eventually disappear resulting in a periodic configuration $\ldots 01010101 \ldots$. Similarly, at $\rho = \frac{2}{3}$ annihilation of all defects results in a periodic configuration $\ldots 110110110 \ldots$. Since these processes can be considered a generalization of a simple ballistic annihilation, one can conjecture that their rate of convergence to equilibrium should be the same as for the ballistic annihilation, in agreement with the results of computer simulations presented in a previous section.

7. Conclusion

We have presented numerical evidence suggesting that, for conservative cellular automata with piecewise linear flow diagrams, relaxation to equilibrium at a critical point follows a universal power law with exponent $-\frac{1}{2}$. The universality of this critical behavior is related to the structure of limit sets of such rules, which can be described as unions of shifts of finite type. At critical points the spatial measure entropy of the limit set goes to zero, which means that the limit set consists of a finite number of configurations. Moreover, the dynamics of such rules can be viewed as interaction of "defects" propagating in opposite directions and annihilating upon collision, just like in a simple ballistic annihilation process, for which the power law $t^{-1/2}$ behavior has been established analytically.

References

[1] D. Chowdhury, L. Santen, and A. Schadschneider, "Statistical physics of vehicular traffic and some related systems," *Physics Reports* **329** (2000) 199–329.
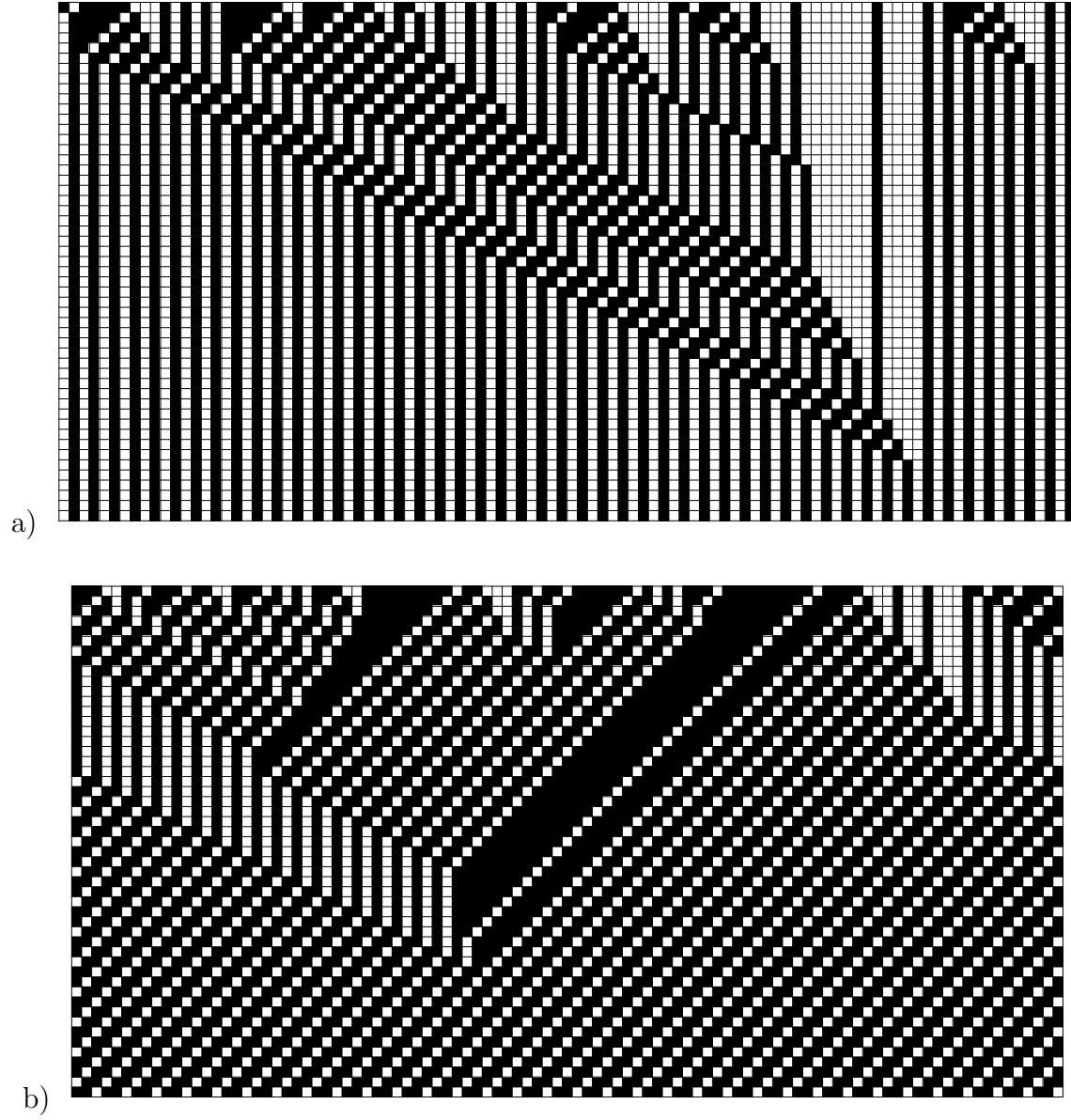
a)

b)

Figure 6: Spatiotemporal diagrams for rule 31633399164 with density of particles a)$\rho = \frac{1}{2}$ and b) $\rho = \frac{2}{3}$.

[2] K. Nagel and H. J. Herrmann, "Deterministic models for traffic jams," *Physica A* **199** (1993) 254–269.

[3] H. Fukś and N. Boccara, "Generalized deterministic traffic rules," *Int. J. Mod. Phys. C* **9** (1998) 1–12, `adap-org/9705003`.

[4] K. Nishinari and D. Takahashi, "Multi-value cellular automaton models and metastable states in a congested phase," *J. Phys. A: Math. Gen.* **33** (2000) 7709–7720.

[5] J. Krug and H. Spohn, "Universality classes for deterministic surface growth," *Phys. Rev. A* **38** (1988) 4271–4283.

[6] T. Nagatani, "Creation and annihilation of traffic jams in a stochastic assymetric exclusion model with open boundaries: a computer simulation," *J. Phys. A: Math. Gen.* **28** (1999) 7079–7088.

[7] K. Nagel, "Particle hopping models and traffic flow theory," *Phys. Rev. E* **53** (1996) 4655–4672.

[8] M. S. Capcarrere, M. Sipper, and M. Tomassini, "Two-state, r=1 cellular automaton that classifies density," *Phys. Rev. Lett.* **77** (1996) 4969–4971.

[9] H. Fukś, "Solution of the density classification problem with two cellular automata rules," *Phys. Rev. E* **55** (1997) 2081R–2084R, `comp-gas/9703001`.

[10] S. Wolfram, *Cellular Automata and Complexity: Collected Papers*. Addison-Wesley, Reading, Mass., 1994.

[11] H. Fukś, "A class of cellular automata equivalent to deterministic particle systems," in *Hyndrodynamics Limits and Related Topics*, S. Feng, A. T. Lawniczak, and S. R. S. Varadhan, eds., Fields Institute Communications Series vol. 27, pp. 57–70. AMS, Providence, RI, 2000.

[12] N. Boccara and H. Fukś, "Cellular automaton rules conserving the number of active sites," *J. Phys. A: Math. Gen.* **31** (1998) 6007–6018, `adap-org/9712003`.

[13] M. Fukui and Y. Ishibashi, "Traffic flow in 1D cellular automaton model including cars moving with high speed," *J. Phys. Soc. Japan* **65** (1996) 1868–1870.

[14] H. Fukś, "Exact results for deterministic cellular automata traffic models," *Phys. Rev. E* **60** (1999) 197–202, `comp-gas/9902001`.

[15] V. Belitsky and P. A. Ferrari, "Invariant measures and convergence for cellular automaton 184 and related processes," `math.PR/9811103`. Preprint.

[16] D. Lind and B. Marcus, *An Introduction to Symbolic Dynamics and Coding*. Cambridge University Press, Cambridge, 1995.

[17] N. Boccara, J. Nasser, and M. Roger, "Particlelike structures and their interactions in spatiotemporal patterns generated by one-dimensional deterministic cellular-automaton rules," *Phys. Rev. A* **44** (1991) 866–875.

[18] Y. Elskens and H. L. Frisch, "Annihilation kinetics in the one-dimensional ideal gas," *Phys. Rev. A* **31** (1985) 3812–3816.